DOI: 10.1002/zaac.200500325

A New Family of Binary Layered Compounds of Platinum with Alkali Metals (A = K, Rb, Cs)

Andrey Karpov and Martin Jansen*

Stuttgart, Germany, Max-Planck-Institut für Festkörperforschung

Received June 17th, 2005.

Abstract. By reacting platinum with alkali metals (A = K, Rb, Cs) a new family of binary alkali metal platinides has been synthesized and characterized by chemical analysis, X-ray powder diffraction, thermal analysis (DTA and DSC), and magnetic measurements. All three compounds exhibit similar XRD-patterns with strong reflections that can be indexed on the basis of a rhombohedral crystal system (K_xPt: a = 2.6462(1), c = 17.123(1); Rb_xPt: a = 2.6415(1) Å, c = 17.871(1) Å; Cs_xPt: a = 2.6505(1) Å, c = 18.536(1) Å; $x < {}^1/_2$). The a lattice constant is independent on the alkali metal used and of value close to the Pt−Pt distance in $NaPt_2$ (2.645 Å). The c parameter increases monotonically with the growing atomic radius of the alkali metal. The average structure of the alloys consists of cubic close packed layers of platinum atoms with layers of disordered alkali metals in between. For all compounds besides the strong reflections small satellites are observed which cannot be indexed together with the rhombohedral peaks in any rational 3-dimensional lattice. However, these satellites can be indexed as incommensurate modulations within the *ab* plane (found propagation vectors k = (0.1011, 0.2506, 0) for Cs_xPt, and k = (0.0168, 0.2785, 0) for Rb_xPt).

Keywords: Alkali metals; Binary alloys; Crystal structure; Intermetallic phases; Platinum

Introduction

Binary intermetallics is one of the most widely investigated classes of inorganic compounds. The Pauling database contains more than 45000 entries covering approximately 2500 binary systems for nonradioactive metals [1]. Several concepts have been developed trying to predict possible existence of an intermetallic compound in a binary system, accounting for different atomic properties of the constituents (size, atomic number, cohesive energy, electrochemical properties, valence electron number) [2]. One concept with a very good agreement between theoretically predicted and experimental findings is the *Miedema's* model which calculates enthalpies of formation of an alloy using two atomic properties − the chemical potential and the electron density at the boundary of the Wigner-Seitz atomic cell [3]. According to this model, among the binary alkali metal − platinum systems, only in Li−Pt and Na−Pt systems stable compounds might be formed. This prediction coincided for a long time with experimental data. In the Li−Pt system four bulk compounds (Li_2Pt [4], LiPt [4], $LiPt_2$ [5], and $LiPt_7$ [6−8]) have been synthesized and characterized, and in the Na−Pt system one compound ($NaPt_2$ [5, 9]) is known. The first evidence for the existence of several compounds in the Cs−Pt system had been observed in [10], however the compositions were not clarified. Recently, we synthesized the first compound in the Cs−Pt system − Cs_2Pt, which remarkably represents an ionic compound exhibiting an open band gap [11]. The relativistic stabilization of the $6s^2$ electronic configuration and atom polarizations are the factors favoring the stability of this binary intermetallic, which were not covered by *Miedema* due to their complexity. In addition, the processes involved in adsorption of alkali metals on platinum surfaces, which act as promoters in many catalyticreactions, have been intensively studied [12]. Several ordered surface structures in Na−Pt(111) and K−Pt(111) systems have been observed with alkali metals occupying threefold *hcp* (hexagonal closed packed) holes [13, 14]. In the present paper we report on a family of isotypic bulk binary phases in the A−Pt systems (A = K, Rb, Cs).

* Prof. Dr. M. Jansen
Max-Planck-Institut für Festkörperforschung
Heisenbergstr. 1
D-70569, Germany
Fax: +49-(0)711-689-1502
E-mail: M.Jansen@fkf.mpg.de

Experimental Part

Starting materials

Rubidium and cesium were prepared from RbCl or CsCl, respectively, by reduction with Ca, and distilled two times in vacuum [15]. Potassium (99 %, Merck, Germany) was purified by filtration of the melt and subsequent distillation (twice) [15].

Platinum sponge (99.9 %, MaTeck, Jülich, Germany), which was used in high temperature reactions with alkali metals (T = 700 °C), was dried and degassed by heating at 400 °C in vacuum ($p \sim 2\times10^{-5}$ mbar). For low temperature reactions with cesium (at 200 < T < 400 °C), very active platinum powder with an average particle size of 100 nm was prepared according to [16] as follows. Typically, 0.5 g of K_2PtCl_4 was suspended in 50 ml of *di*-ethylene

glycol (DEG) at intensively stirring, and the suspension was heated at 120 °C for 1 hour. Then the suspension was allowed to cool down to room temperature and centrifuged. The mother solution of KCl in DEG was decanted, while the residual black platinum powder was washed twice and resuspended in ethanol, with intermediate centrifugations. Finally, the platinum was dried overnight at room temperature in vacuum of 10^{-3} mbar. The as prepared platinum was studied by scanning electron microscopy equipped with an integrated *EDAX*-EDX system, and not even traces of oxygen, or other impurity elements were detected.

Tantalum tubes, typically used as reaction containers, were cleaned with dilute HF (~5 %), thoroughly rinsed with water, and heated at 1100 °C in high vacuum for 12 hours (final vacuum at the maximal temperature of $\sim 2\times10^{-5}$ mbar). For low-temperature reactions of cesium with platinum (at $T < 400$ °C), a platinum tube was used as purchased.

Because of the extreme sensitivity to air and moisture of both, reagents and products, all operations were performed under strictly inert conditions using Schlenk technique or in an Ar-filled glovebox with humidity and oxygen levels both lower than 0.1 ppm (MB 150B-G-II, M.Braun, Germany).

Sample preparation

Potassium and rubidium platinides. For the syntheses of potassium and rubidium platinides (K_xPt and Rb_xPt, $x < {}^1/_2$), the corresponding alkali metals and platinum sponge were weighted out in different atomic ratios (A:Pt = 1:1 to 3:1, A = K, Rb), and placed into tantalum tubes, which were sealed under argon with an arc welder. In order to prevent oxidation, the tantalum tubes were encapsulated under argon in silica jackets, carefully dried with a flame. The reaction mixtures were heated with a rate of 50 °C/h to 700 °C, annealed at this temperature for two days, and then cooled down to room temperature with a rate of 10 °C/h. Independently of the atomic ratios used, unreacted alkali metals were contained in the raw products at all times, and it was not possible to fill a capillary for powder X-ray investigations, at this step. For characterisation of the products, the excesses of alkali metals were removed by distillation in vacuum at appropriate temperatures during appropriate times (e.g. rubidium was completely removed by heating the mixtures at 130 °C overnight in a vacuum of 10^{-3} mbar, the excess of potassium was removed by heating the mixtures at 250 °C overnight in a vacuum of 10^{-3} mbar). The resulting powders are light grey with small shiny crystallites.

Cesium platinide. At the same conditions, reaction of cesium with platinum following by distillation of cesium at 100 °C in vacuum of 10^{-3} mbar leads to the product, light-grey shiny Cs_xPt ($x \sim {}^1/_2$), containing red transparent crystals of Cs_2Pt as a by-product [11]. Heating the resulting mixture at higher temperatures ($T > 150$ °C) in vacuum leads to decomposition of Cs_2Pt, however, the product phase Cs_xPt ($x < {}^1/_2$) was now contaminated by elemental platinum. Cs_xPt, free of Cs_2Pt and Pt, was obtained by reaction of cesium with self-prepared platinum powder at $T < 400$ °C. For example, a mixture of cesium with platinum in a ratio 2.1:1 was placed under argon in a Pt-crucible. The latter was closed mechanically with a nipper, and encapsulated in a carefully dried Pyrex tube, long enough that one end stuck out of the furnace. The tube was heated at 300 °C for 2 weeks. In the Pt-crucible a black powder was obtained, while the excess of cesium condensed in the cold part of the glass tube. So it was possible to characterise the as obtained powder without additional distillation of cesium.

Sample characterization

Chemical analyses. Chemical compositions of the samples were determined using ICP-OES (Vista Pro, Varian, Darmstadt, Germany). Heavy atom analyses were also performed using a scanning electron microscope (XL 30 TMP, Philips, Holland, tungsten cathode, 25 kV), equipped with an integrated *EDAX*-EDX system.

Laboratory X-ray Powder Diffraction. All samples were routinely examined by X-ray powder diffraction. Powder patterns were collected with a linear position-sensitive detector on a STADI P diffractometer in Debye-Sherrer geometry (Stoe & Cie GmbH, Germany, Ge-monochromated $CuK\alpha_1$ radiation, $\lambda = 1.5406$ Å, $5 < 2\Theta < 100$ degrees, or $MoK\alpha_1$ radiation, $\lambda = 0.7093$ Å $4 < 2\Theta < 40$ degrees, in steps of 0.01 degree), with the samples sealed in glass capillaries of 0.2 mm diameter. The data were calibrated with respect to an external Si-standard. To investigate thermal stability of the products, high temperature X-ray diffraction patterns were collected at temperatures up to 500 °C in steps of 50 °C (the accuracy of the temperature is ±5 °C) on a STADI P diffractometer in Debye-Sherrer geometry equipped with a heating tool (Stoe & Cie GmbH, Germany, Ge-monochromated $MoK\alpha_1$, $\lambda = 0.7093$ Å, $4 < 2\Theta < 40$ degrees, in steps of 0.01 degree) with the specimens sealed in quartz capillaries of 0.2 mm diameter.

High resolution X-ray powder diffraction. High resolution X-ray powder diffraction data of the rubidium and cesium platinides were collected at ambient conditions in transmission geometry with the samples sealed in a 0.3 mm capillaries at beamline ID31 at the European Synchrotron Radiation Facility (ESRF) (Si(111) monochromator, 9-Ge(111) crystal analyzers, $\lambda = 0.32696$ Å, 9 scintillation counters, $0.5° < 2\Theta < 38.0°$ in steps of $0.002° 2\Theta$).

Thermal properties. Differential scanning calorimetry (DSC) was performed with a computer-controlled DSC sensor (DSC 404 C Pegasus, Netzsch GmbH, Germany). Differential thermal analysis (DTA) and thermo-gravimetry were conducted on a computer-controlled thermal analyzer (STA 409, Netzsch GmbH, Germany). Powder samples (typically 20 mg) were placed in platinum (for DSC) or corundum (for DTA-TG) crucibles with lids, heated to 600 °C with a rate of 10 °C/min, and then cooled down to room temperature with the same rate. The whole process was run under argon.

Magnetic measurements. Magnetisation, exemplary of rubidium and cesium platinides, was measured using a SQUID magnetometer (MPMS 5.5, Fa., Quantum Design, USA) in the temperature range 5 − 330 K at $H = 1$, 3 and 5 T. The specimens (109.1 mg of $Rb_{0.33}Pt$ and 80.8 mg of $Cs_{0.5}Pt$) were sealed in silica tubes under helium. The raw data were corrected for the holder contribution. A small field dependency was corrected by extrapolation of χ values to $1/H \rightarrow 0$.

Results and Discussion

General Properties

By reacting the constituting elements, a new family of binary alkali metal platinides with general composition A_xPt (A = K, Rb, Cs, $x < {}^1/_2$) has been discovered. They crystallize as light grey shiny crystals in a shape of hexagonal plates, some tens of micrometers in size, thus we have not succeeded in picking suitable crystals for X-ray single crystal investigations. The compounds hydrolyse rapidly when

exposed to air. According to ICP-OES and EDX analyses the chemical composition depends strongly on the respective temperature of distillation of the alkali metal excesses. However, in all cases the maximum alkali metal content did not exceed one half of the platinum content. The lowest borders of the homogeneity range are not yet well defined. Major difficulties arise from the dependency of the contents on the p/T conditions at the removal of excesses of alkali metals. For K_xPt the lowest potassium to platinum ratio x, observed so far, was 0.29, for Rb_xPt, x was more than 0.33, while for Cs_xPt it was at all times close to 0.5. According to DSC, DTA-TG and high temperature diffraction measurements, the compounds are thermally stable in argon up to 400−550 °C (the K−Pt phase up to 540 °C, the Rb−Pt phase up to 450 °C, and the Cs−Pt phase up to 420 °C), thereafter they melt incongruently evolving alkali metals. In vacuum the thermal stability appears to shift to lower temperatures. In several preliminary transmission electron microscopy experiments, conducted at room temperature, evaporation of the alkali metals as nanometer size crystallites was observed, at exposing the substances to an electron beam. All compounds are diamagnetic at room temperature (330 K: $\chi(Rb_{0.33}Pt) = -7.61\times10^{-8}$ emu/g, $\chi(Cs_{0.5}Pt) = -1.41\times10^{-7}$ emu/g). The magnetic susceptibility of the rubidium sample shows a temperature dependency as a consequence of its contamination with the elemental platinum.

Crystal Structure

All compounds exhibit virtually isotypic XRD-patterns. The strong reflections for all three compounds can be indexed on the basis of a rhombohedral crystal system (Fig. 1−3, Table 1). The parameter a of the resulting hexagonal cells is almost independent on the type alkali metal incorporated, and ~2.64 Å of value which is too small as compared to the smallest separations possible for the respective alkali metal atoms ($2r$(K) = 4.60 Å, $2r$(Rb) = 4.94 Å, $2r$(Cs) = 5.34 Å [17, p. 47]) or even the alkali metal ions ($2r(K^+)$ = 2.76 Å, $2r(Rb^+)$ = 3.04 Å, $2r(Cs^+)$ = 3.34 Å, all values for CN (coordination number) = 6, [17, p. 49]).When comparing the length of the a lattice constants with the shortest Pt−Pt distance of elemental platinum (d(Pt−Pt) = 2.77 Å [18]), it can be noted that it is significantly shorter. Assuming a full occupation of the platinum positions the reduction of a as compared to d(Pt−Pt) in elemental platinum could be ascribed to additional, covalent interactions, similarly to those observed in the one-dimensional homoatomar platinum chains of BaPt (d(Pt−Pt) = 2.71 Å [19]). A similar contraction to d(Pt−Pt) = 2.645 Å has been observed in $NaPt_2$ (Laves phase), where platinum atoms are coordinated by six platinum atoms and six sodium atoms in the shape of an icosahedron [9]. The c lattice parameter, and thus the corresponding inter-layer distance $c/3$, increases monotonically with the growing atomic radius of the alkali metal (Fig. 4, Table 1), however appears to be independent on the alkali metal content.

Placing the alkali metals in the octahedral holes of the platinum *ccp* (cubic closed packed) sub-lattice − which

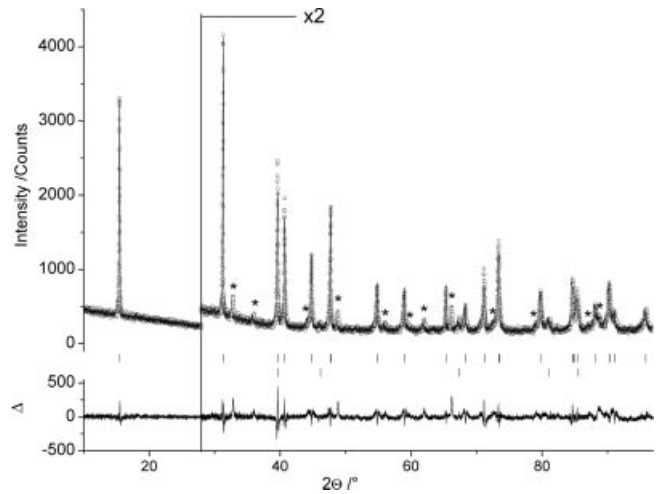

Fig. 1 Observed powder X-ray diffraction pattern (CuKα_1 radiation, λ = 1.5406 Å) for $K_{0.4}Pt$, and a calculated Le-Bail fit with peak indexing on the basis of a rhombohedral crystal system (R_p = 7.52 %, R_{wp} = 11.31 %, GOF = 1.64, all values as defined in JANA2000 [22]). Shown are the observed (circles) and calculated (solid line) data and the enlarged difference curve between observed and calculated profiles (in an additional window). Vertical lines indicate the Bragg reflection positions for $K_{0.4}Pt$ (top) and Pt (bottom). Stars indicate not indexed satellite reflections. The high angle part is enlarged for clarity.

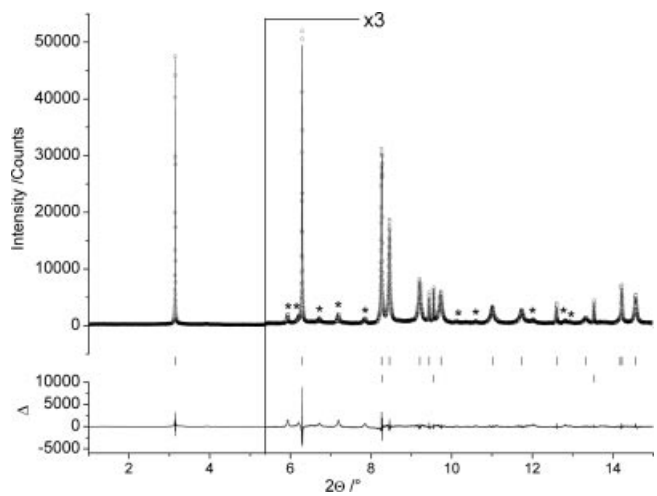

Fig. 2 Observed high resolution synchrotron powder X-ray diffraction pattern (λ = 0.32696 Å) for $Rb_{0.33}Pt$, and a calculated Le-Bail fit with peak indexing on the basis of a rhombohedral crystal system (R_p = 10.94 %, R_{wp} = 15.95 %, GOF = 3.22, all values as defined in JANA2000 [22]). Shown are the observed (circles) and calculated (solid line) data and the enlarged difference curve between observed and calculated profiles (in an additional window). Vertical lines indicate the Bragg reflection positions for $Rb_{0.33}Pt$ (top) and Pt (bottom). Stars indicate not indexed satellite reflections. The high angle part is enlarged for clarity.

corresponds to the position most distant from Pt − one can deduce the maximal possible space (in atomic radii, r_{max}) available within the alkali metals in the platinides ($r_{max}(A_{A_xPt}) = \sqrt{(\sqrt{3}a/3)^2 + (c/6)^2} - a/2$; $r_{max}(K_{K_{0.4}Pt}) =$ 1.91 Å, $r_{max}(Rb_{Rb_{0.33}Pt}) = 2.03$ Å, $r_{max}(Cs_{Cs_{0.5}Pt}) = 2.12$ Å). The minimal alkali metal radii can be estimated assuming completely disordered layers of the alkali metals between the platinum layers ($r_{min}(A_{A_xPt}) = (c/3 - a)/2$; $r_{min}(K_{K_{0.4}Pt}) = 1.53$ Å, $r_{min}(Rb_{Rb_{0.33}Pt}) = 1.66$ Å, $r_{min}(Cs_{Cs_{0.5}Pt}) = 1.76$ Å). The ranges of "allowed" (within the Pt sublattice) alkali metal radii thus fall into the range between the respective ionic radii and atomic radii in metals. As is quite obvious, for all compounds a significant reduction of the alkali metal as compared to the atomic radii in metals is observed, suggesting a considerable degree of their ionization. Noteworthy, the arithmetic means of the estimated range of tolerable alkali metal radii in the platinides is getting closer to the ionic radii when moving from potassium through rubidium to cesium, in full accordance with the trend of their first ionization potentials. A similar conclusion can be drawn comparing the volume of $Cs_{0.5}Pt$ per formula unit ($V_{Cs_{0.5}Pt} = 37.56$ Å^3, assuming $Z = 3$) with the volume increments as reported by *Biltz* [20] for the ionic and metallic radii ($V_{Cs^+_{0.5}Pt} = 22.04$ Å^3, $V_{Cs_{0.5}Pt} = 41.99$ Å^3).

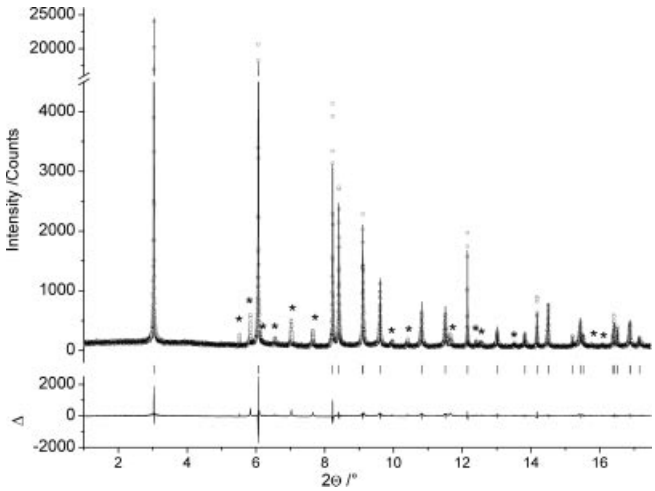

Fig. 3 Observed high resolution synchrotron powder X-ray diffraction pattern ($\lambda = 0.32696$ Å) for $Cs_{0.5}Pt$, and a calculated Le-Bail fit with peak indexing on the basis of a rhombohedral crystal system ($R_p = 16.86$ %, $R_{wp} = 22.02$ %, GOF = 2.73, all values as defined in JANA2000 [22]). Shown are the observed (circles) and calculated (solid line) data and the enlarged difference curve between observed and calculated profiles (in an additional window). Vertical lines indicate the Bragg reflection positions for $Cs_{0.5}Pt$. Stars indicate not indexed satellite reflections. The intensity scale is interrupted between 4500 and 16000 counts, for clarity.

Table 1 Lattice parameters of the alkali metal platinides for the rhombohedral substructures.

Formula	a /Å	c /Å	0.333·c /Å	V /Å^3	0.333·V /Å^3
$K_{0.4}Pt$	2.6462(1)	17.123(1)	5.708(-)	103.839(5)	34.613(-)
$Rb_{0.33}Pt$	2.6415(1)	17.871(1)	5.957(-)	107.991(2)	35.997(-)
$Cs_{0.5}Pt$	2.6505(1)	18.536(1)	6.179(-)	112.768(2)	37.589(-)

Table 2 d values and relative intensities of the reflections which were not indexed on the basis of the rhombohedral subcell or were assigned to the impurity of the elemental platinum.

	$K_{0.4}Pt$		$Rb_{0.33}Pt$		$Cs_{0.5}Pt$
d /Å	I /%	d /Å	I /%	d /Å	I /%
2.726	9.6	3.156	1.39	3.390	1.07
2.490	5.8	3.018	1.22	3.209	2.50
2.043	5.0	2.789	0.93	3.076	3.30
1.863	6.4	2.606	1.41	2.858	0.85
1.638	4.1	2.387	0.88	2.667	2.08
1.549	3.9	1.851	0.54	2.448	1.36
1.495	4.7	1.770	0.55	1.881	0.70
1.411	7.2	1.562	0.80	1.800	0.70
1.210	3.8	1.464	0.67	1.611	1.11
1.116	3.9	1.451	0.53	1.513	0.64
1.102	5.6			1.497	0.59
				1.389	0.52
				1.194	0.45
				1.169	0.44

By inspecting the full-widths of half-maxima (FWHM) of the powder reflections a strong anisotropy can be detected. The *00l* and *hh0* peaks have three to six times smaller full-widths at the same 2Θ as compared to the peaks with one non-zero h index (Fig. 5). This is giving strong evidence for a significant disorder of this layered structure within the *ab* plane.

Besides the rhombohedral reflections discussed above, a series of peaks with low intensities has been observed in all samples. Their positions and relative intensities are listed in Table 2. In trying to index them together with the rhombohedral reflections, we have failed finding any rational 3-dimensional lattice. In a second approach, we have tried to assign these peaks to a propagation vector using the program SUPERCELL of the program package FULLPROF2000 [21] assuming incommensurate modulations in the *ab* plane (the reciprocal component z^* of the propagation vector was fixed to 0). The best solution we found

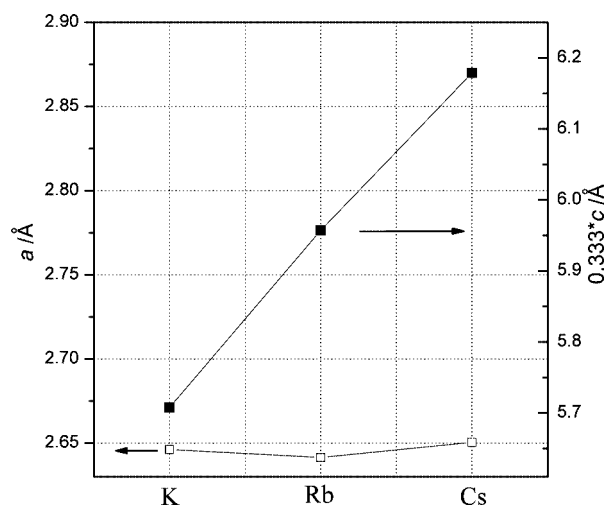

Fig. 4 The dependence of the a (left y-axis) and $c/3$ (right y-axis) lattice constants of A_xPt on the alkali metal.

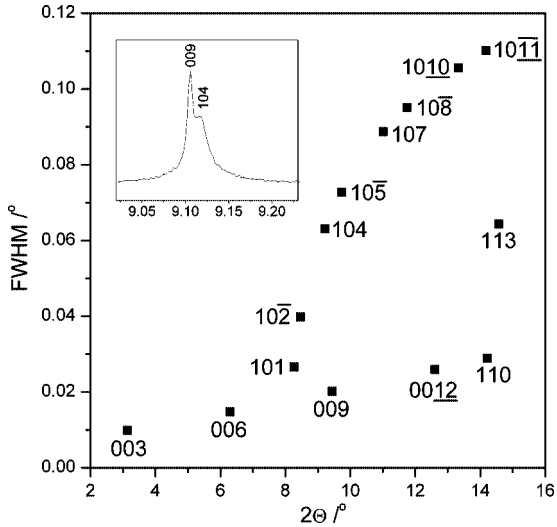

Fig. 5 FWHM *versus* diffraction angle 2Θ for $Rb_{0.33}Pt$. The observed XRD-profiles of *009* and *104* reflections for $Cs_{0.5}Pt$ are shown in the insert window, demonstrating the difference between their shapes.

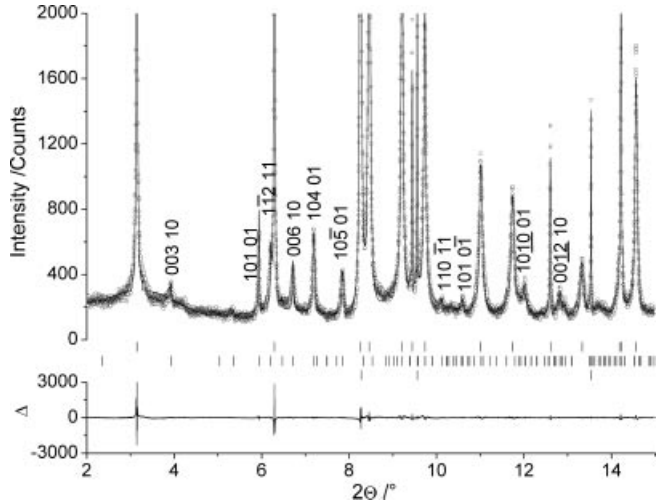

Fig. 6 A Le-Bail fit for $Rb_{0.33}Pt$ according to the 5-dimensional indexing (propagation vector k = (0.0168, 0.2785, 0), R_p = 7.99 %, R_{wp} = 10.29 %, GOF = 2.08, all values as defined in JANA2000 [22]). Shown are the observed (circles) and calculated (solid line) data and the enlarged difference curve between observed and calculated profiles (in an additional window). Vertical lines indicate the Bragg reflection positions for $Rb_{0.33}Pt$ on the basis of a rhombohedral crystal system (top), incommensurately modulated satellite reflections (middle) and Pt (bottom). Satellite reflections with non-zero intensities are labelled with five indices.

for $Cs_{0.5}Pt$ was k = (0.1011, 0.2506, 0). For $Rb_{0.33}Pt$ the best k was found to be (0.0168, 0.2785, 0) c.f. Fig. 6. No solutions have been found with propagation vectors along the c or a axes only (keeping $h,k = 0$, or $k,l = 0$, respectively). Attempts to find any propagation vector for $K_{0.4}Pt$ from laboratory powder X-ray diffraction data failed probably due to an insufficient resolution of the satellite peaks. The different propagation vectors found for the compounds are more likely an effect of the different alkali metal radii rather than of the different stoichiometry. Attempts to determine the supercell using electron diffraction have failed, so far, due to the low stability of the samples under an electron beam.

At analyzing the average crystal structures we placed platinum atoms at the unit cell's origin (0,0,0). When moving from cesium through rubidium to potassium the difference between the calculated XRD-patterns of the platinum sublattice and measured XRD-patterns becomes lower, because of the decreasing scattering contribution of the alkali metals as compared to those of platinum. The main disagreement is observed for the ratio of intensities of the (0,0,3) to (0,0,6) reflections (c.f. Fig. 7). The subsequent difference Fourier syntheses in several space groups ($R3$, $R\bar{3}$, $R3m$, $R\bar{3}m$) did not reveal any maxima with electron densities comparable to the scattering factors of the corresponding alkali metal. This points out partial occupation of crystallographic positions by alkali metals in rhombohedral space groups. Optimizing occupation factors we found the best coincidence between calculated and measured XRD-patterns with alkali metals building disordered bilayers at z = 1/6 ± 1/24 in centrosymmetrical space groups ($R\bar{3}$, $R\bar{3}m$), or a monolayer at z = 1/6 in non-centrosymmetrical space groups ($R3$, $R3m$). In the case of centrosymmetrical space groups the alkali metals fill space at too small distances from the platinum atoms as compared to the sum of their ionic or metallic radii. Hence these space groups can be ruled out. The structure solutions in the non-centrosymmetrical space groups, however, give plausible estimations for the alkali metal radii as discussed above. Fig. 8 shows a Rietveld plot for rubidium platinide using a model of disordered rubidium layers centered between the *ccp* platinum layers (space group $R3m$, Pt at 3*a* (0,0,0), Occ. (occupation factor) = 1, Rb1 at 18*c* (0,1/3,1/6), Occ. = 0.056, Rb2 at 3*a* (0,0,1/6), Occ. = 0.056, Rb2 at 3*a* (1/3,2/3,1/6), Occ. = 0.056, Rb2 at 3*a* (2/3,1/3,1/6), Occ. = 0.056, total chemical composition $Rb_{0.5}Pt$, Fig. 9). Besides differences related to the satellite reflections, a quite good coincidence between the calculated and measured XRD-patterns was thus achieved.

Conclusions

New binary alloys of platinum with alkali metals (A = K, Rb, Cs) have been synthesized. In a first approximation, the crystal structure of the compounds can be described consisting of *ccp* platinum layers with a Pt−Pt distance of ~2.64 Å separated by disordered and partly occupied alkali metal layers. A significant reduction of the Pt−Pt separation as compared to those in the elemental platinum (2.77 Å) can be assigned to covalent interactions as earlier in the case of BaPt [19]. The estimated alkali metal radii are considerably reduced as compared to the atomic alkali metal radii, thus suggesting ionization of the alkali metals

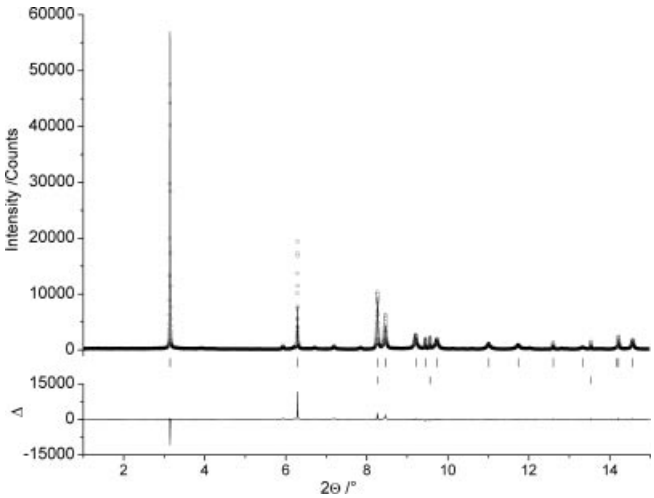

Fig. 7 A Rietveld fit of "$Rb_{0.5}Pt$" using a model with only platinum atoms at the unit cell's origin (R(all) = 11.53 %, R_w(all) = 12.78 %, R_p = 17.45 %, R_{wp} = 22.90 %, GOF = 4.62, all values as defined in JANA2000 [22]). For labelling see Fig. 2.

with transfer of part of the charge to the platinum. Hence, the alloys can be considered as further members of platinides − compounds consisting of negatively charged platinum ions.

However, some problems with the superstructure solution, arising from a series of small satellite reflections, remain not settled yet. The peaks have been indexed using modulation vectors within the *ab* plane but the modulated structure has not been solved. Unfortunately due to the low stability of the samples in vacuum our preliminary attempts to make transmission electron microscopy have failed, so far. The possible way to overcome this problem might be in conducting TEM experiments at cooling with liquid nitrogen. Another approach to solve the modulated structure might be to grow single crystals under high pressure − this procedure was already successfully applied for the growth of single crystals constituted of one component with a low melting point and a second with a high melting point, e.g. $NaPt_2$ [9].

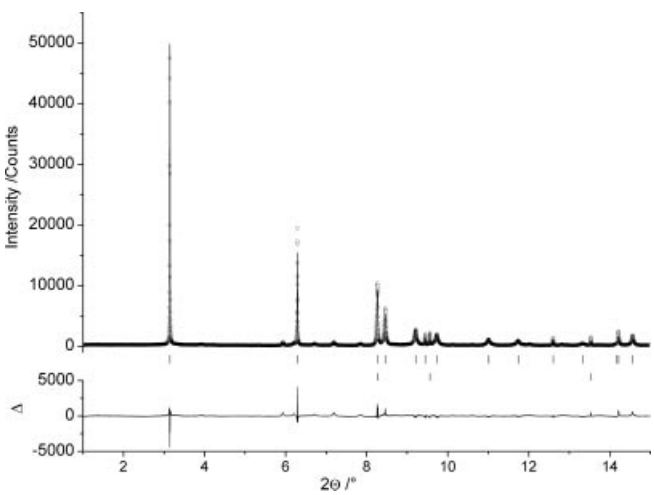

Fig. 8 A Rietveld fit of "$Rb_{0.5}Pt$" using a model with platinum atoms at the unit cell's origin and rubidium atoms forming disordered layers in the middle between the platinum layers (R(all) = 5.12 %, R_w(all) = 4.57 %, R_p = 12.80 %, R_{wp} = 17.05 %, GOF = 3.45, all values as defined in JANA2000 [22]). For labelling see Fig. 2.

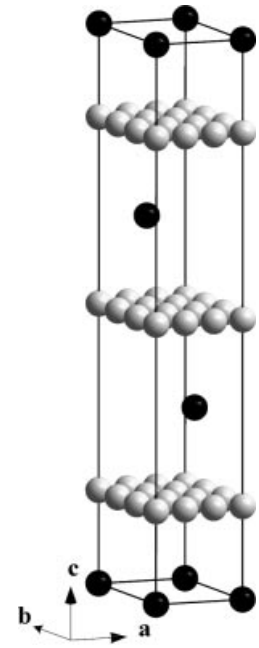

Fig. 9 Crystal structure of "$Rb_{0.5}Pt$" as refined by Rietveld profile fitting (black spheres: platinum atoms; light grey spheres: rubidium atoms; black lines: unit cell-edges).

Acknowledgement. The authors would like to thank *Claus Mühle* for the assistance at the experimental work, *Marie-Luise Schreiber* for the chemical analysis, *Priv. Doz. Dr. Robert E. Dinnebier* and *Dr. Andy Fitch* for performing the high resolution X-ray powder diffraction measurements, *Eva Brücher* for the magnetic measurements.

References

[1] Pauling File, Inorganic Materials Database and Design System, Binary Edition, Ed.-in-chief P. Villars, Version 1.0, Release 2002/1.
[2] P. Villars in *Intermetallic Compounds Principles and Practice*, Eds. J. H. Westbrook, R. L. Fleischer, John Wiley Sons, Chichester, U.K., 1994, Vol. 1, p. 227−275.
[3] F. R. de Boer, R. Boom, W. C. M. Mattens, A. R. Miedema, A. K. Niessen in *Cohesion in Metals, Transition Metal Alloys*, Eds. F. R. de Boer, D. G. Pettifor, Cohesion and Structure, North-Holland Physics Publishing, Amsterdam, 1988, Vol. 1.
[4] W. Bronger, B. Nacken, K. Ploog, *J. Less-Common Met.* **1975**, *43*, 143.
[5] C. P. Nash, F. M. Boyden, L. D. Whittig, *J. Am. Chem. Soc.* **1960**, *82*, 6203.
[6] W. Bronger, W. Klemm, *Z. Anorg. Allg. Chem.* **1962**, *319*, 58.
[7] O. Jr. Loebich, C. J. Raub, *J. Less-Common Met.* **1980**, *70*, P47.

[8] W. Bronger, G. Klessen, P. Müller, *J. Less-Common Met.* **1985**, *109*, L1.
[9] K.-J. Range, F. Rau, U. Klement, *Acta Crystallogr. C* **1989**, *45*, 1069.
[10] M. Jansen, A.-V. Mudring, *Diploma Thesis*, A.-V. Mudring, Rheinische Friedrich-Wilhelms-Universität, Bonn, 1995.
[11] A. Karpov, J. Nuss, U. Wedig, M. Jansen, *Angew. Chem.* **2003**, *115*, 4966; *Angew. Chem. Int. Ed.* **2003**, *42*, 4818.
[12] H. P. Bonzel in *Physics and Chemistry of Alkali Metal Adsorption*, Eds. H. P. Bonzel, A. M. Bradshaw, G. Ertl, Elsevier, Amsterdam, 1989.
[13] J. B. Hannon, M. Giesen, C. Klinker, G. Schulze Icking-Konert, D. Stapel, H. Ibach, J. E. Müller, *Phys. Rev. Lett.* **1997**, *78*, 1094.
[14] S. Moré, A. P. Seitsonen, W. Berndt, A. M. Bradshaw, *Phys. Rev. B* **2001**, *63*, 075406.
[15] G. Brauer, *Handbuch der Präparativen Anorganischen Chemie*, Bd. 2, Ferdinand Enke Verlag, Stuttgart, 1978, p. 938−942.
[16] L. K. Kukihara, G. M. Chow, P. E. Schoen, *NanoStructured Mat.* **1995**, *5*, 607.
[17] U. Müller, *Anorganische Strukturchemie*, B. G. Teubner, Stuttgart, 1996.
[18] H. E. Swanson, E. Tatge, *J. Res. Nat. Bur. Stand.* **1951**, *46*, 318.
[19] A. Karpov, J. Nuss, U. Wedig, M. Jansen, *J. Am. Chem. Soc.* **2004**, *126*, 14123.
[20] W. Biltz, *Raumchemie der festen Stoffe*, Verlag von Leopold Voss, Leipzig, 1934.
[21] J. Rodriguez-Carvajal, FULLPROF Version Juli 2001, CEA/Saclay, France, 2001.
[22] V. Petricek, M. Dusek, Jana2000, Version 21/10/2003. The crystallographic computing system, Institute of Physics, Praha, Czech Republic, 2000.

